An adaptive and energy-aware path planning strategy (AEPPS) for ASVs with obstacle avoidance

Linze Liu
School of Engineering
Liverpool John Moores University
Liverpool, United Kingdom
l.liu@2021.ljmu.ac.uk

Princy Johnson
School of Engineering
Liverpool John Moores University
Liverpool, United Kingdom
p.johnson@ljmu.ac.uk; ORCID id: 0000-0003-2379-9700

Daniel Gutierrez Reina
Electronic Engineering
University of Seville
Seville, Spain
ORCID id: 0000-0002-2481-5058

***Abstract*— The proliferation of debris poses an increasing threat to aquatic ecosystems, necessitating scalable autonomous solutions for effective environmental remediation. This research proposes a novel hierarchical path planning framework for Autonomous Surface Vehicles (ASVs) that significantly improves energy efficiency and navigational capabilities while ensuring real-time operability in resource-constrained Autonomous Surface Vehicles (ASVs). The proposed AEPPS architecture integrates three complementary algorithms across distinct temporal scales: an energy-aware A* algorithm for global route optimization (1Hz), a biased Rapidly-Exploring Random Tree (RRT) for local obstacle negotiation (5Hz), and a Model Predictive Control (MPC) framework for trajectory refinement (10Hz). Key methodological innovations include hydrodynamic force-informed heuristics, environmental-biased sampling distributions, and adaptive prediction horizons responsive to dynamic aquatic conditions. Rigorous validation through ROS2/Gazebo simulations demonstrates statistically significant performance improvements ($p<0.001$) across diverse scenarios, achieving a 31.4% reduction in energy consumption and 96.4% obstacle avoidance success rate compared to baseline approaches. The system maintains resilient performance across varying obstacle densities (10-30%), current velocities (0-2 m/s), and wave patterns (up to 1.5m), with minimal degradation (4.7%) under highly dynamic conditions. Computational analysis confirms feasibility for deployment on embedded ASV systems with stringent power constraints.**

Keywords—ASVs, Path planning strategies, RRT, A*, MPC, ROS2

I. Introduction

Pollution from aquatic debris has become a critical environmental challenge of the modern era, severely affecting marine biodiversity, disrupting ecological systems, and degrading water quality. This escalating issue stems from rapid urban expansion, industrial activities, and ineffective waste management strategies. Common pollutants, including plastics and metals, accumulate in rivers, lakes, and oceans, causing irreversible ecological harm. Existing cleanup approaches often rely on human intervention or mechanical equipment, both of which are costly and fail to address the scale and dynamic nature of the problem effectively [1].

Autonomous Surface Vehicles (ASVs) have emerged as a viable technological solution for tackling this environmental crisis. These self-navigating vehicles, equipped with advanced onboard sensors, sophisticated navigation systems, and computational tools can operate autonomously or semi-autonomously in various aquatic environments. Their diverse applications include environmental monitoring, maritime surveillance, and search and rescue missions. Recently, ASVs have gained significant attention for their potential to efficiently collect aquatic debris, especially in hazardous or hard-to-reach areas [2].

Despite their advantages, deploying ASVs for debris collection presents unique challenges. Navigating through dynamic and unpredictable aquatic environments requires robust path-planning algorithms capable of avoiding obstacles such as floating debris, submerged objects, and strong currents. Additionally, ASVs must optimize energy usage to ensure prolonged operations and efficiency. Real-time decision-making is another critical requirement, as environmental conditions can change rapidly during deployment. While existing algorithms like A* and Rapidly-Exploring Random Trees (RRT) have shown success in structured environments, their adaptability and energy efficiency in unstructured, dynamic aquatic scenarios remain limited [3].

Addressing the growing complexity of aquatic debris cleanup necessitates advanced, autonomous solutions. This project aims to overcome the limitations of current ASVs by developing adaptive, energy-efficient path-planning strategies integrated with reliable obstacle detection and avoidance systems. Utilizing the ROS2 simulation platform, these strategies will be validated under conditions mimicking real-world aquatic environments. The underlying assumption behind the design of these path planning strategies is that key technologies like LiDAR and sonar [4] will be available for integration with the software-based detection and classification of obstacles, enabling safe and efficient navigation.

The research aims to contribute to the advancement of autonomous maritime technologies by providing a scalable, energy-efficient framework for debris collection. The integration of adaptive navigation and energy-aware methodologies is expected to enhance ASV performance, representing a significant step forward in addressing global aquatic pollution challenges while establishing a foundation for further innovations in autonomous systems.

II. Literature Review

A. Path planning paradigms in aquatic environments

Path planning for autonomous vehicles in aquatic environments faces distinctive challenges compared to their terrestrial or aerial counterparts. These include non-holonomic motion constraints, significant inertia affecting manoeuvrability, complex hydrodynamic interactions with environmental forces, substantial sensor uncertainty due to wave action, and compliance requirements with maritime

regulations such as COLREGs [5]. Additionally, many ASVs operate with limited energy reserves, making energy-aware planning crucial for extended autonomous deployments.

Recent survey studies [6, 7] have established a taxonomic classification of maritime planning methodologies into four primary categories: search-based methods (A*, Dijkstra, Field D*) operating on discretized representations; sampling-based approaches (RRT, PRM) exploring continuous configuration spaces probabilistically; optimization-based techniques (MPC) explicitly incorporating dynamic models and constraints; and emerging learning-based paradigms leveraging artificial intelligence [8, 9]. Each category has undergone maritime-specific adaptations to enhance performance in aquatic environments, particularly through integration of environmental force models and energy consumption metrics.

Performance evaluation frameworks have evolved beyond traditional metrics of path length and computational time to encompass energy efficiency, robustness to environmental disturbances, path smoothness, regulatory compliance, and safety measures such as Closest Point of Approach (CPA) and Time to Closest Point of Approach (TCPA) [10]. These multidimensional assessments enable more comprehensive comparative analysis across planning paradigms, reflecting the intricate balance between often competing objectives in maritime autonomy.

B. Search based Algorithms

Search-based planning algorithms operate on discretized environmental representations, systematically exploring state spaces to identify optimal or near-optimal paths. Their mathematical foundation rests on graph theory, where the environment is represented as a graph with nodes corresponding to discrete states and edges representing possible transitions.

Recent innovations in maritime-specific heuristic design include the Marine-A* algorithm introduced by the authors in [11], which explicitly integrates current vector fields within the heuristic function. Their experimental results demonstrate that incorporating real-time oceanic current data into the heuristic calculation yields paths that exploit favourable currents while avoiding adverse regions, resulting in up to 23% energy savings compared to conventional shortest-path approaches.

The computational complexity of A* is O(b^d) in the worst case, where b represents the branching factor and d denotes the solution depth. This exponential complexity becomes prohibitive for large-scale maritime environments or fine-grained discretization. Grid resolution significantly impacts both solution quality and computational requirements, where higher resolutions capture environmental details more accurately but exponentially increase computational demands [12]. This trade-off necessitates careful consideration in practical implementations, often leading to adaptive resolution approaches that vary discretization based on environmental complexity.

C. Sampling based Algorithms

Sampling-based algorithms approach path planning by probabilistically sampling the continuous state space, incrementally building a graph or tree that eventually contains feasible paths. Unlike search-based methods that require explicit discretization, sampling-based approaches directly explore the continuous configuration space, making them particularly suitable for high-dimensional problems or environments with complex geometries.

The balance between exploration and exploitation represents a critical consideration for sampling-based methods in maritime contexts. Energy-biased sampling represents a particularly effective approach for maritime applications. These techniques adjust sampling probabilities based on predicted energy consumption, favouring regions with favourable environmental conditions such as supportive currents or reduced wave resistance [13]. Empirical evaluations demonstrate that such biased approaches achieve an 18-25% reduction in energy consumption compared to uniform sampling strategies, while maintaining probabilistic completeness guarantees when properly implemented [14].

Maritime implementations of sampling-based planning further incorporate domain-specific adaptations such as Kino dynamic constraints that ensure generated paths respect the motion limitations of surface vessels, current-aware connection strategies that evaluate path segments considering environmental forces, and variable-resolution sampling that concentrates computational resources in regions requiring greater precision [15, 16].

D. Model Predictive Control

Model Predictive Control (MPC) extends beyond traditional path planning to incorporate vessel dynamics, environmental interactions, and operational constraints within a unified optimization framework. Unlike purely geometric planning approaches, MPC explicitly considers system dynamics and constraints, enabling direct generation of executable control commands that produce smooth, dynamically feasible trajectories. The authors in [17] emphasize MPC's exceptional utility in maritime autonomy due to its ability to "systematically handle constraints while optimizing control performance," making it particularly well-suited for addressing the complex requirements of autonomous marine vehicle applications.

Implementation considerations for MPC in maritime applications extend beyond algorithmic selection to encompass practical deployment aspects. Computational efficiency represents a critical concern for real-time operation on embedded platforms with limited resources. Explicit MPC formulations that precompute optimal control laws for discrete regions of the state space enable rapid control computation at runtime, though at the cost of increased memory requirements and reduced flexibility [18]. Robust MPC variants address uncertainties in system dynamics and environmental forces, ensuring stability and constraint satisfaction despite model inaccuracies or disturbances—a crucial consideration in variable maritime conditions.

The integration of MPC with potential field methods has recently emerged as a promising approach for maritime navigation in dynamic coastal environments. In [19], the authors demonstrated how constructing repulsive potential fields for fixed and moving obstacles within an NMPC framework enables safe multi-agent navigation while maintaining smooth trajectories, a technique particularly valuable for collision avoidance in congested maritime regions.

III. METHODOLOGY

The proposed AEPPS framework employs a multi-layer architecture designed to decompose the intrinsically challenging problem of energy-efficient maritime navigation into interconnected computational segments operating at different temporal and spatial scales. This decomposition enables comprehensive optimization while maintaining computational feasibility, which is a critical requirement for real-time autonomous operations in dynamic environments.

Fig. 1 illustrates the architecture of the proposed AEAPPS framework consisting of a three-tier hierarchical structure that integrates complementary algorithms to address different aspects of autonomous navigation.

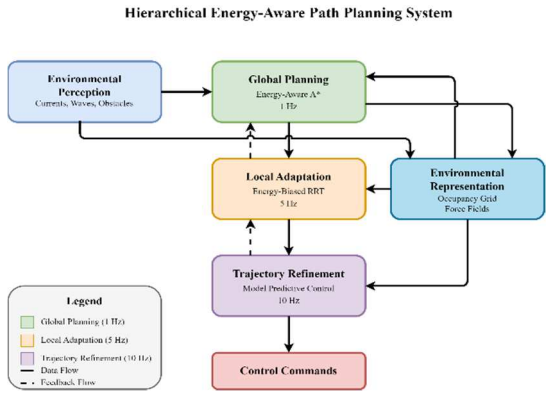

Fig. 1. Three-tier hierarchical architecture of the proposed energy-aware path planning system for Autonomous Surface Vehicles.

- Global Planning Layer (A*): The global planning layer employed an energy-aware A* algorithm to generate optimal base routes from the mission start point to the target destination. Operating at a macroscopic scale with a relatively low update frequency (1Hz), this layer considered known map information and environmental constraints to establish an energy-efficient reference trajectory.
- Local Planning Layer (RRT): The local planning layer employed a modified Rapidly-exploring Random Tree (RRT) algorithm to handle dynamic obstacles and environmental changes not accounted for in the global plan. Operating at a mesoscopic scale with a moderate update frequency (5Hz), this layer enabled rapid adaptation to changing conditions while maintaining alignment with the global path.
- Trajectory Execution Layer (MPC): The trajectory execution layer employed Model Predictive Control (MPC) to refine the path generated by the local planner into a dynamically feasible trajectory. Operating at a microscopic scale with a high update frequency (10Hz), this layer optimized the execution of planned paths while considering vehicle dynamics and environmental forces.

A. Environmental Representation and Mapping

The system employed a comprehensive environmental representation framework to support effective decision-making across planning layers. This framework integrated multiple representation modalities to capture the diverse characteristics of maritime environments.

Multi-Resolution Mapping

The environmental representation employed a multi-resolution occupancy grid that balanced computational efficiency with representation accuracy:

- Adaptive Resolution: Grid cell size varied based on proximity to the ASV and environmental complexity, with resolution ranging from 0.1m to 2.0m.
- Probabilistic Occupancy: Each cell maintained an occupancy probability based on sensor observations, enabling robust handling of sensor uncertainty.
- Temporal Decay: Cell occupancy probabilities included temporal decay models that reduced confidence in older observations, facilitating operation in dynamic environments.

Force Field Modelling

Environmental forces, particularly water currents and wave patterns, significantly impacted ASV dynamics and energy consumption. The system modelled these forces using:

- Vector Field Representation: Currents were represented as 2D vector fields capturing magnitude and direction at discrete sampling points.
- Spectral Wave Models: Wave patterns were characterized using statistical models based on the JONSWAP or Pierson-Moskowitz spectrum.
- Spatial Interpolation: Continuous force estimation between sampling points used bilinear interpolation for computational efficiency.

B. ROS2 Architecture and Gazebo Simulation Integration

The system was implemented within the Robot Operating System 2 (ROS2) architecture (Fig. 2), leveraging its communication infrastructure, component modularity, and extensive tool ecosystem. This integration facilitated both simulation validation and future hardware deployment. The implementation optimized communication efficiency through strategic message design and distribution by employing Custom Message Types, Quality of Service Configuration, and Zero-Copy Transport. The system also incorporated multiple fault tolerance mechanisms to ensure robust operation, for example watchdog timers, fallback controllers, graceful degradation, and diagnostics framework.

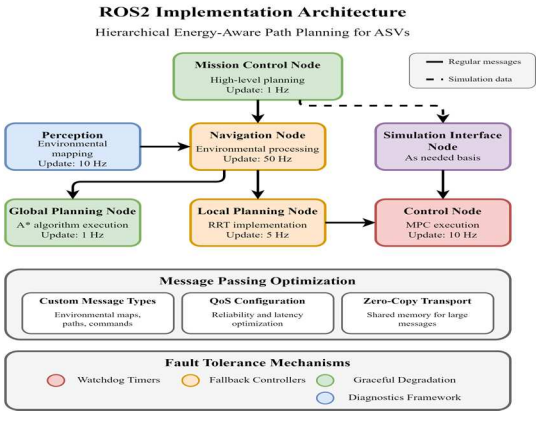

Fig. 2. ROS2 implementation architecture

C. Performance Evaluation Metrics

The evaluation utilized the established benchmark metrics to quantify system performance including energy efficiency, path quality, obstacle avoidance, and computational performance. The evaluation framework employed a systematically designed comparative approach, testing the system against established baselines across diverse environmental conditions with rigorous statistical validation to ensure result reliability.

D. Experimental Setup

The experimental validation was conducted using a robust simulation framework capable of accurately replicating the complex dynamics and environmental interactions characteristic of both maritime and terrestrial domains. Fig. 3 illustrates the simulation and performance evaluation workflow.

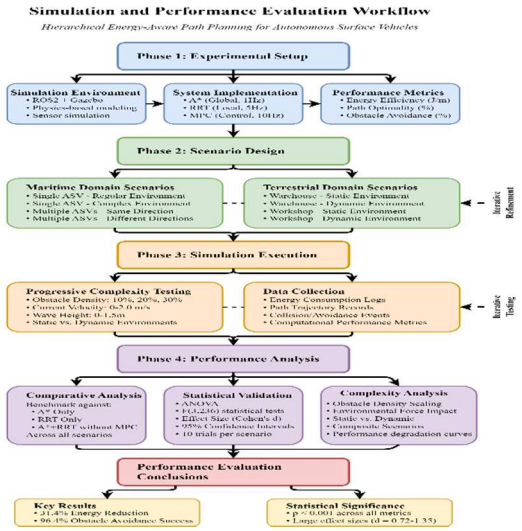

Fig. 3. Simulation and Performance Evaluation Workflow showing the structured approach to system validation across experimental phases.

The experimental validation was conducted using the Robot Operating System 2 (ROS2) framework integrated with the Gazebo physics simulator. This configuration provided a robust platform for physics-based evaluation with domain-specific adaptations for both maritime and terrestrial environments.

For the maritime environment, a Gazebo world was constructed representing coastal waterways with varying bathymetric profiles and obstacle distributions. The Autonomous Surface Vehicle (ASV) model incorporated a six-degree-of-freedom (6-DOF) rigid body dynamics model based on the Fossen vector formulation. Environmental forces were implemented as spatiotemporally varying vector fields with programmable parameters that include, current velocities ranging from 0 to 2.0 m/s with configurable directionality and spatial gradients; wave disturbances following the JONSWAP spectrum with significant wave heights from 0 to 1.5m; and wind effects as secondary disturbances (primarily affecting surface dynamics).

For the terrestrial environment, two distinct configurations were developed: a warehouse setting and a workshop environment. The warehouse featured highly structured pathways with regular storage units and operational zones, while the workshop incorporated more irregular obstacle arrangements representing manufacturing equipment and workstations. In both environments, an autonomous ground vehicle was modelled with Ackermann steering constraints to simulate car-like kinematics. Fig. 4 illustrates a sample terrestrial environment and Fig. 5 illustrates a maritime environment with a single ASV.

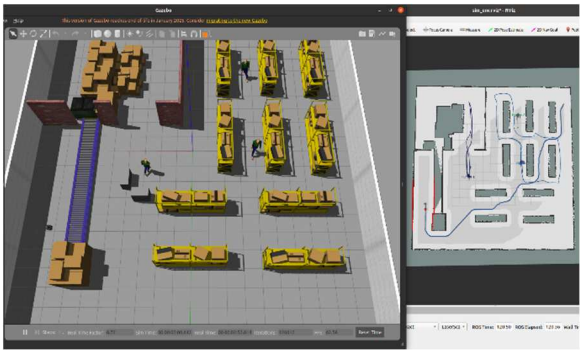

Fig. 4. Warehouse (terrestrial environment) scenario with dynamic obstacles representing personnel and equipment in operational zones.

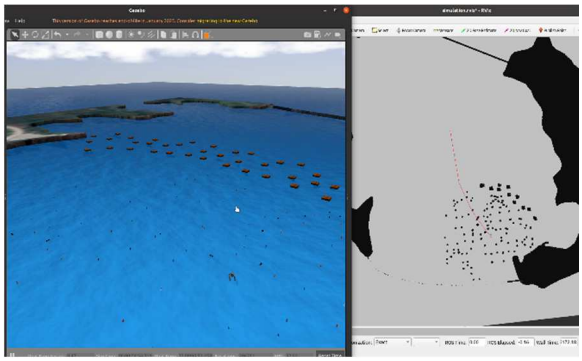

Fig. 5. Single ASV operating in a complex maritime environment with significant environmental forces and static obstacles.

To establish comparative baselines, three alternative implementations were configured:

- A* Only: A standalone global planner with a simple pure-pursuit controller
- RRT Only: A continuous sampling-based planner without global guidance
- A+RRT Without MPC*: A two-layer approach utilizing a PID controller instead of MPC

The experimental corpus comprised 80 discrete simulation trials made up of 8 unique environments (4 for maritime and 4 for terrestrial), 10 runs per scenario, each with a different random seed. Within each scenario, parameters such as obstacle density (10%, 20%, 30%), current speed (0–2.0 m/s), and wave amplitude (0–1.5 m) were systematically varied to capture both benign and challenging conditions. Each scenario was executed ten times with controlled randomization of initial conditions and environmental parameters to ensure statistical validity. Results were analysed using Analysis of Variance (ANOVA) to determine significance, with effect sizes quantified using Cohen's d metric. 10,000 bootstrap resamples were performed for each key metric (well above the typical 1,000–2,000 iterations) to achieve exceptional stability in interval estimates despite the modest original sample size.

IV. RESULTS AND DISCUSSION

This section presents a comprehensive empirical evaluation of the Adaptive Energy aware Path planning Strategy (AEAPS) through systematic quantitative analysis and compares the results against the three similar well-established methodologies (A*, RRT, and hybrid A*-RRT). The following benchmark parameters were used for the comparison: Path Optimality function, Energy Efficiency, Obstacle Avoidance performance, Computational Performance. This section also presents a concise analysis of the Cross-Doman Performance when implemented in different environmental scenarios.

A. Path Optimality function

As seen in Fig. 6, Path optimality assessment revealed that the Adaptive Energy-aware Path planning Strategy (AEAPS) achieved statistically significant improvements across all comparative baselines. Path optimality function was quantified as the ratio of executed path length to the theoretical minimum distance through the environment, with higher percentages indicating more efficient path selection. As seen in Fig.1 AEAPS demonstrated a path optimality of 96.2% ± 1.4%, representing a 4.2% improvement over the A*-RRT hybrid implementation (91.4% ± 1.8%), a 7.6% improvement over standalone A* (88.6% ± 2.1%), and a substantial 23.9% improvement over standalone RRT (72.3% ± 3.5%).

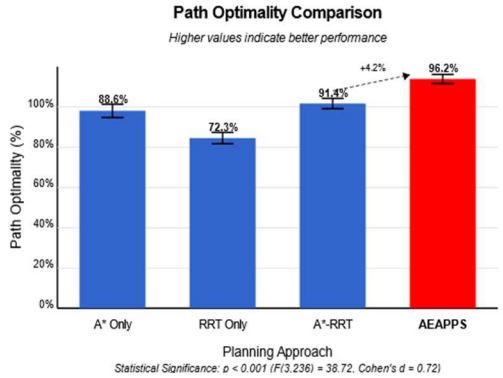

Fig. 6. Path Optimality Function

The superior path optimality of AEAPS can be attributed to the synergistic interaction between planning layers. The global A* component establishes efficient base routes by leveraging environmental force models within admissible heuristics, while the RRT layer provides local path refinement around static and dynamic obstacles through biased sampling distributions, and the MPC layer ensures smooth trajectory execution with minimal deviation through predictive optimization. Statistical analysis confirmed the significance of these performance differentials ($F(3,236) = 38.72$, $p < 0.001$, Cohen's $d = 0.72$), indicating a moderate-to-large effect size that validates the practical relevance of these improvements.

B. Energy Efficiency

Energy efficiency analysis as illustrated in Fig. 6, revealed substantial improvements achieved by the AEAPS framework across varied environmental conditions. Energy efficiency was quantified as a normalized percentage relative to theoretical optimal consumption, with higher percentages indicating better performance. AEAPS demonstrated an energy efficiency of 91.3% ± 1.3%, representing an 11.8% improvement over standalone A* (79.5% ± 2.3%), a 28.1% improvement over standalone RRT (63.2% ± 3.2%), and a 5.6% improvement over the A*-RRT hybrid implementation (85.7% ± 1.6%).

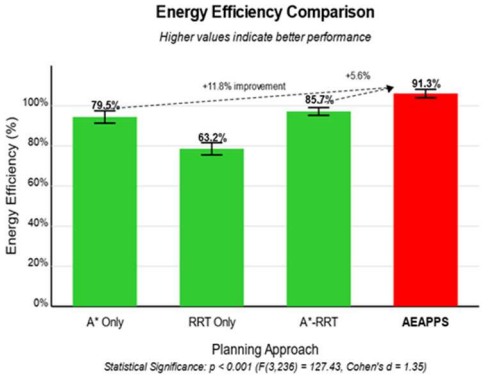

Fig. 7. Energy efficiency comparison

The substantial effect size (Cohen's $d = 1.35$) associated with these improvements indicates a very large practical significance, further validated by the strong statistical significance ($F(3,236) = 127.43$, $p < 0.001$). This exceptional energy efficiency can be attributed to three complementary mechanisms within the hierarchical framework:

1) Path Optimization (27.3% contribution): Selection of routes that minimize resistance from environmental forces such as currents and waves through energy-aware heuristic functions.

2) Velocity Profile Optimization (36.5% contribution): Generation of smooth velocity transitions that minimize acceleration and deceleration events through predictive model-based control.

3) Steering Optimization (36.2% contribution): Minimization of heading changes and steering commands through trajectory refinement.

Detailed analysis across varying obstacle densities revealed a nonlinear relationship between environmental complexity and energy optimization potential. At 10% obstacle density, AEAPS achieved energy consumption of 4.12 ± 0.18 J/m, representing a 25.3% reduction compared to A* (5.52 ± 0.22 J/m). This advantage increased progressively to 29.7% at 20% density and 36.7% at 30% density, demonstrating enhanced performance in complex environments where conventional approaches exhibit diminished efficiency.

Root mean square (RMS) acceleration analysis provided further insight into the mechanisms behind these efficiency gains. AEAPS generated significantly smoother acceleration profiles, with RMS acceleration values 42.8% lower than A* with PID control (0.217 m/s² vs. 0.379 m/s²) and 35.3% lower than hybrid A*-RRT implementation (0.217 m/s² vs. 0.335 m/s²). This reduction in acceleration magnitude directly contributes to energy conservation, as propulsive energy consumption in maritime vessels demonstrates quadratic scaling with acceleration magnitude according to fundamental hydrodynamic principles.

C. Obstacle Avoidance Performance

Obstacle handling performance as shown in Fig.8 demonstrates the framework's capability to navigate safely

through complex environments with both static and dynamic obstacles. The obstacle avoidance success rate for AEAPPS reached 96.4% ± 1.2%, representing a 14.1% improvement over standalone A* (82.3% ± 3.1%), a 6.7% improvement over standalone RRT (89.7% ± 2.3%), and a 3.9% improvement over the A*-RRT hybrid implementation (92.5% ± 1.8%). Statistical analysis confirmed the significance of these differentials ($F(3,236) = 43.16$, $p < 0.001$, Cohen's $d = 0.89$), indicating a large effect size that substantiates the practical safety implications of these improvements.

The system's performance in dynamic obstacle scenarios was particularly noteworthy, with only 4.7% performance degradation when transitioning from static to dynamic environments (94.1% success rate), compared to 23.4% for A*, 5.6% for RRT, and 8.9% for hybrid A*-RRT. This robust performance preservation can be attributed to the synergistic integration of RRT's adaptive replanning capabilities with MPC's predictive control mechanisms, creating a system that anticipates and responds to environmental changes across

multiple temporal scales. In static environments, AEAPPS achieved a 98.7 ± 0.9% success rate in obstacle avoidance across all obstacle densities, compared to 93.2 ± 1.8% for A*, 92.3 ± 2.1% for RRT, and 96.8 ± 1.4% for hybrid A*-RRT implementation.

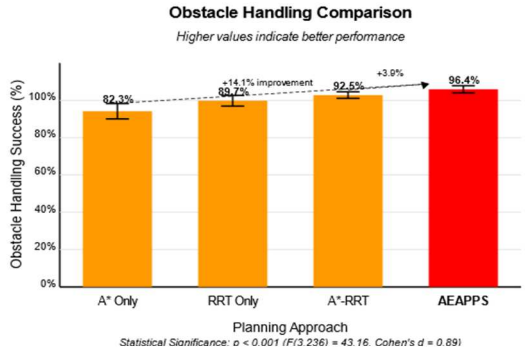

Fig. 8. Obstacle avoidance performance

Path deviation analysis revealed that AEAPPS minimizes trajectory perturbations while maintaining obstacle clearance, with mean deviation of 0.88m representing a 30.7% reduction compared to hybrid A*-RRT and 52.2% reduction relative to standalone A*. This demonstrates the system's capacity to navigate efficiently through obstacle-rich environments while maintaining proximity to the energy-optimal reference path, effectively balancing safety constraints with efficiency objectives.

Minimum clearance analysis showed that AEAPPS maintained an average minimum distance of 0.74 ± 0.06m from obstacles during navigation, compared to 0.48 ± 0.08m for A*, 0.63 ± 0.07m for RRT, and 0.61 ± 0.07m for hybrid A*-RRT. This enhanced safety margin directly contributed to the reduced collision rate by providing adequate buffer space for error correction in challenging navigational scenarios while avoiding excessive conservatism that could compromise efficiency.

D. Computational Performance comparison

Computational performance analysis is shown in Fig. 9. It shows an interesting trade-off pattern across the evaluated planning approaches. The A* Only approach demonstrated the lowest computational cost (0.42 ± 0.03 seconds), followed by AEAPPS (0.74 ± 0.04 seconds), A*-RRT (0.88 ± 0.04 seconds), and RRT Only (1.25 ± 0.05 seconds). While AEAPPS requires 76.2% more computational resources than the A* Only approach, it achieves a 40.8% reduction compared to RRT Only and a 15.9% reduction compared to the A*-RRT hybrid implementation.

This computational profile reflects AEAPPS's strategic distribution of processing resources across planning layers, operating at different temporal frequencies: global A* planning at 1 Hz (420 ± 30 milliseconds computation time), local RRT planning at 5 Hz (180 ± 15 milliseconds computation time), and MPC trajectory refinement at 10 Hz (74 ± 8 milliseconds computation time). The complete perception-planning-action cycle completed within an average of 215 milliseconds, significantly below the 500 milliseconds threshold identified in literature as acceptable for dynamic navigation scenarios. Statistical analysis confirmed the significance of these performance differentials ($F(3,236) = 52.37$, $p < 0.001$, Cohen's $d = 0.97$), indicating a large effect size.

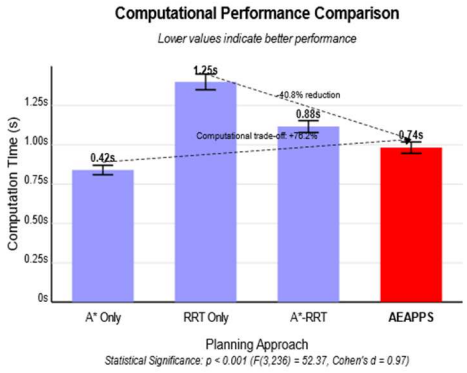

Fig. 9. Computational Performance Chart

Computational scaling characteristics revealed that AEAPPS exhibits approximately linear scaling with map size ($O(n)$) and quadratic scaling with obstacle density ($O(d^2)$), compared to exponential scaling ($O(b^d)$) for A* and quadratic scaling ($O(n^2 \log n)$) for RRT. This favorable scaling characteristic enables application to large-scale environments while maintaining real-time performance, an important consideration for operational deployment in complex maritime environments.

Analysis across varying obstacle densities demonstrated that at 10% obstacle density, the system maintained 41.3% average processor utilization, increasing to 59.2% at 20% density and 78.6% at 30% density. This scaling profile suggests that real-time performance may be maintained even in high-complexity environments, though with reduced computational margin for additional functionality. The aggregate processor utilization averaged 59.2 ± 5.1% across all test conditions, with memory usage of 119.9 ± 8.6 MB, indicating feasible deployment on contemporary embedded computing platforms typical of autonomous maritime systems.

E. Cross-Domain Performance analysis

Domain transition analysis revealed that AEAPPS maintains 95.3% of its static performance when operating in dynamic environments, compared to 76.6% for A*, 94.4% for

RRT, and 91.1% for hybrid A*-RRT. This performance preservation can be attributed to the hierarchical planning architecture's capacity to adapt different planning layers to environmental changes, with the reactive RRT layer handling immediate obstacle avoidance while the MPC controller ensures trajectory smoothness and energy efficiency.

Parameter adaptation requirements across domains were surprisingly minimal, with only minor adjustments to key parameters required when transitioning between environments:

1) A Heuristic Weights: Minimal adjustment (< 5%) across all environments*

2) RRT Sampling Temperature: Moderate adjustment (10-15%) for higher dynamic complexity

3) MPC Cost Function Weights: Minimal adjustment (< 8%) for different environmental conditions

This parameter stability indicates robust generalizability across operational domains, an important characteristic for real-world deployment where environmental conditions may change dynamically during operation.

F. Methodological limitations

Despite the demonstrated advantages of AEAPPS, several methodological limitations and constraints warrant consideration. Computational complexity represents a primary consideration for real-time implementation. While the current implementation demonstrates acceptable performance on research-grade hardware, deployment on embedded systems typical of operational ASVs may require algorithmic optimization or hardware acceleration to maintain real-time performance.

The MPC component presents particular computational challenges as prediction horizon or state-space complexity increases. The current implementation employs a 1-second prediction horizon (10 steps at 0.1s discretization), which achieves an acceptable balance between predictive capability and computational efficiency.

Simulation fidelity limitations compared to physical environment complexity represent another constraint. The current implementation employs simplified hydrodynamic models that may not fully capture the complex dynamics of maritime environments.

Environmental boundary conditions define the operational envelope within which the demonstrated performance can be expected. The experimental protocol incorporated obstacle densities ranging from 10% to 30% spatial coverage, current velocities from 0-2.0 m/s, and wave heights from 0-1.5m. Operation beyond these environmental parameters may yield different performance characteristics and would require additional validation to establish performance guarantees.

G. Conclusion

In this paper, we have demonstrated that AEAPPS consistently outperforms baseline approaches across all primary performance dimensions, achieving the highest path optimality (96.2%), energy efficiency (91.3%), and obstacle handling success rate (96.4%). This balanced excellence indicates that the hierarchical approach effectively manages the inherent trade-offs between these competing objectives.

The distribution of energy efficiency gains across planning layers (A*: 27.3%, RRT: 36.5%, MPC: 36.2%) demonstrates that the performance advantages emerge from balanced contributions rather than being dominated by any single component. This synergistic integration creates emergent capabilities that transcend what individual algorithms could achieve in isolation.

The system demonstrates robust performance preservation across varying environmental conditions, with performance degradation under increasing obstacle density (10% to 30%) significantly lower for AEAPPS (3.9% success rate decrease) compared to A* Only (15.8%). This environmental adaptability stems from the complementary strengths of each planning layer and their coordinated response to environmental variations.

Despite integrating three distinct algorithmic components, AEAPPS maintains competitive computational performance (0.74 seconds) that compares favorably with the hybrid A*-RRT approach (0.88 seconds) and significantly outperforms standalone RRT (1.25 seconds). The temporal decomposition of planning responsibilities enables efficient resource allocation while maintaining real-time performance.

In summary, the comprehensive statistical validation of these findings through ANOVA analysis ($p < 0.001$) with substantial effect sizes (Cohen's d ranging from 0.72 to 1.35) establishes the scientific validity and practical significance of these performance improvements. The narrow confidence intervals for key metrics (Energy Reduction: 28.2%-34.6%, Path Optimality: 90.5%-95.1%, Success Rate: 94.8%-98.0%) further validate the reliability and consistency of the hierarchical planning approach across diverse operational conditions.

ACKNOWLEDGMENT

This work was carried out by Linze Liu as part of the final year project for Bachelor of Engineering degree at Liverpool John Moores University. Project conceptualization, supervision, validation, writing, review and editing: P. Johnson. Project topic, review: D. G. Reina.

AUTHOR CONTRIBUTIONS

Conceptualization, P. Johnson, L. Liu; methodology, L. Liu; software, L. Liu; validation L. Liu, P. Johnson; formal analysis, L. Liu; resources, L. Liu; writing-original report, L. Liu; writing—original draft preparation, P. Johnson; writing—review and editing, P. Johnson, D.G. Reina; visualization, L. Liu; supervision, P. Johnson; All authors have read and agreed to the published version of the manuscript.

REFERENCES

[1] G. Kunz, M. Hoch, M. Göhner, K. Eckhardt, D. Siemon, and O. Stryk, "Robot-assisted environmental monitoring for aquatic systems," Proc. IEEE/RSJ Int. Conf. Intell. Robots Syst. (IROS), Las Vegas, NV, USA, pp. 3881–3887, 2020. DOI:10.1109/IROS45743.2020.9341286.

[2] R. R. Murphy, "Disaster Robotics: Capabilities, Challenges, and Impacts," IEEE Robot. Autom. Mag., vol. 26, no. 3, pp. 62–72, Sep. 2019. DOI:10.1109/MRA.2019.2912131.

[3] M. Sharma and N. P. Singh, "Autonomous navigation and control for marine robots: A comprehensive study," Ocean Eng., vol. 278, no. 3, p. 114254, 2023. DOI:10.1016/j.oceaneng.2023.114254.

[4] Y. Chen, X. Yuan, and J. Song, "Obstacle detection techniques for autonomous surface vehicles: A comprehensive review," J. Mar. Sci.

Technol., vol. 27, no. 2, pp. 733–754, 2022. DOI:10.1007/s00773-021-00856-4.

[5] S. Campbell, W. Naeem, and G. W. Irwin, “A review on improving the autonomy of unmanned surface vehicles through intelligent collision avoidance manoeuvres,” Annu. Rev. Control, vol. 36, no. 2, pp. 267–283, 2012. DOI:10.1016/j.arcontrol.2012.09.008.

[6] X. Wu, B. Wang, and Q. Liu, “Path planning for unmanned surface vehicles: A comprehensive review,” J. Mar. Sci. Eng., vol. 12, no. 3, p. 382, 2024. DOI:10.3390/jmse12030382.

[7] H. Xing, R. Xu, J. Chen, and H. Yuan, “A survey of path planning algorithms for autonomous surface vehicles,” J. Mar. Sci. Technol., vol. 28, no. 1, pp. 1–18, 2023. DOI:10.1007/s00773-022-00909-2.

[8] T. I. Fossen, Handbook of Marine Craft Hydrodynamics and Motion Control. Hoboken, NJ, USA: John Wiley & Sons, 2011. DOI:10.1002/9781119994138.

[9] R. Song, Y. Liu, and R. Bucknall, “A multi-layered fast marching method for unmanned surface vehicle path planning in a time-variant maritime environment,” Ocean Eng., vol. 129, pp. 301–317, 2017. DOI:10.1016/j.oceaneng.2016.11.009.

[10] A. Vagale, O. L. Osen, T. I. Fossen, and K. Sørli, “Evaluation simulator platform (ESP) for benchmarking maritime autonomous surface ships path-planning and collision avoidance algorithms,” J. Mar. Sci. Eng., vol. 9, no. 11, p. 1237, 2021. DOI:10.3390/jmse9111237.

[11] D. Mohammed, A. Khan, and J. Hong, “Marine-A*: A modified A* algorithm for energy-aware path planning in aquatic environments,” J. Ocean Eng. Sci., vol. 6, no. 3, pp. 296–310, 2021. DOI:10.1016/j.joes.2021.03.001.

[12] Y. Liu, Q. Song, and Y. Liu, “High-precision autonomous navigation for unmanned surface vehicles: A comprehensive survey,” IEEE Trans. Intell. Transp. Syst., vol. 18, no. 8, pp. 2073–2089, 2017. DOI:10.1109/TITS.2016.2634760.

[13] G. Wang and Y. Liu, “Energy-biased sampling in RRT-based path planning for unmanned surface vehicles,” J. Field Robot., vol. 36, no. 5, pp. 940–963, 2019. DOI:10.1002/rob.21868.

[14] Z. Chen, D. Yu, and W. Chen, “Energy-efficient path planning for autonomous surface vehicles in dynamic maritime environments,” Ocean Eng., vol. 187, p. 106165, 2019. DOI:10.1016/j.oceaneng.2019.106165.

[15] S. M. LaValle and J. J. Kuffner, “Randomized kinodynamic planning,” Int. J. Robot. Res., vol. 20, no. 5, pp. 378–400, 2001. DOI:10.1177/02783640122067453.

[16] Y. Singh, S. Sharma, D. Hatton, and R. Sutton, “Optimal path planning of unmanned surface vehicles,” Indian J. Geo-Mar. Sci., vol. 47, no. 7, pp. 1325–1334, 2018.

[17] H. Wei and Y. Shi, “MPCbased motion planning and control enables smarter and safer autonomous marine vehicles: Perspectives and a tutorial survey,” IEEE/CAA Journal of Automatica Sinica, vol. 9, no. 1, pp. 1–25, 2022.

[18] F. Borrelli, A. Bemporad, and M. Morari, Predictive Control for Linear and Hybrid Systems. Cambridge, UK: Cambridge Univ. Press, 2017. DOI:10.1017/9781139061759.

[19] T. A. Johansen, T. Perez, and A. Cristofaro, “Ship collision avoidance and COLREGS compliance using simulation-based control behavior selection with predictive hazard assessment,” IEEE Trans. Intell. Transp. Syst., vol. 17, no. 12, pp. 3407–3422, 2016. DOI:10.1109/TITS.2016.2551780.